



LUND UNIVERSITY

Improving Code Diversity on Block-Fading Channels by Spatial Coupling

ul Hassan, Najeeb; Lentmaier, Michael; Andriyanova, Iryna; Fettweis, Gerhard

Published in:
[Host publication title missing]

2014

[Link to publication](#)

Citation for published version (APA):

ul Hassan, N., Lentmaier, M., Andriyanova, I., & Fettweis, G. (2014). Improving Code Diversity on Block-Fading Channels by Spatial Coupling. In *[Host publication title missing]* IEEE - Institute of Electrical and Electronics Engineers Inc..

Total number of authors:
4

General rights

Unless other specific re-use rights are stated the following general rights apply:

Copyright and moral rights for the publications made accessible in the public portal are retained by the authors and/or other copyright owners and it is a condition of accessing publications that users recognise and abide by the legal requirements associated with these rights.

- Users may download and print one copy of any publication from the public portal for the purpose of private study or research.
- You may not further distribute the material or use it for any profit-making activity or commercial gain
- You may freely distribute the URL identifying the publication in the public portal

Read more about Creative commons licenses: <https://creativecommons.org/licenses/>

Take down policy

If you believe that this document breaches copyright please contact us providing details, and we will remove access to the work immediately and investigate your claim.

LUND UNIVERSITY

PO Box 117
221 00 Lund
+46 46-222 00 00

Improving Code Diversity on Block-Fading Channels by Spatial Coupling

Najeeb ul Hassan[†], Michael Lentmaier[‡], Iryna Andriyanova^{*}, and Gerhard P. Fettweis[†]

[†]Vodafone Chair Mobile Communications Systems, Dresden University of Technology (TU Dresden), Dresden, Germany, {najeeb_ul.hassan, fettweis}@tu-dresden.de

[‡]Dept. of Electrical and Information Technology, Lund University, Lund, Sweden, michael.lentmaier@eit.lth.se

^{*}ETIS group. ENSEA/UCP/CNRC-UMR8501, 95014 Cergy-Pontoise, France, iryna.andriyanova@ensea.fr

Abstract—Spatially coupled low-density parity-check (SC-LDPC) codes are considered for transmission over the block-fading channel. The diversity order of the SC-LDPC codes is studied using density evolution and simulation results. We demonstrate that the diversity order of the code can be increased, without lowering the code rate, by simply increasing the coupling parameter (memory) of a SC-LDPC code. For a (3,6)-regular SC-LDPC code with rate $R = 1/2$ and memory $m_{cc} = 4$ a remarkable diversity of $d = 10$ is achieved without the need for any specific code structure. The memory of the SC-LDPC codes makes them robust against a non-stationary mobile-radio environment. The decoding of SC-LDPC codes using a latency constrained sliding window decoder is also considered.

I. INTRODUCTION

The mobile-radio channel can be modelled as a slow, flat fading together with additive noise. In many cases, the channel coherence time is much longer than one symbol duration. Thus several symbols are affected by the same fading coefficient. An example of such a channel model is the *block-fading* channel introduced in [1]. In block-fading channel, coded information is transmitted over a finite number of fading blocks to provide *diversity*. The diversity order of the code is an important parameter that gives the slope of the word error rate (WER) of the decoder. Codes achieving diversity equal to the number of fading blocks in a codeword are said to be full diversity codes. In [2], a family of LDPC block codes, called *root-LDPC* codes, are proposed that provide full diversity over a block-fading channel. The root-LDPC codes have a special check node structure called *rootcheck*. Full diversity is provided to the systematic information bits by connecting only one information bit to every rootcheck.

In this paper, we consider spatially coupled low-density parity-check (SC-LDPC) codes for block-fading channels based on the following two observations,

- Convolutional codes, in general, are known to be suitable for transmission over block-fading channels and the diversity can be increased by increasing the constraint length of the code [3].

This work was supported in part by the DFG in the CRC 912 HAEC, European Social Fund in the framework of the Young Investigators Group 3DCSI, and by the European Commission in the framework of the FP7 Network of Excellence in Wireless COMMunications NEWCOM# (Grant agreement no. 318306).

- Root-LDPC codes provide full diversity for the information bits. However, designing root-LDPC codes with diversity order greater than 2 requires codes with rate less than $1/2$. The special structure of the codes makes it a complicated task to generate good root-LDPC codes with high diversity (and thus low rate).

Since SC-LDPC codes have a convolutional structure, they are expected to have a good performance over block-fading channels. In this paper, we present density evolution outage probabilities [2] for random LDPC block and SC-LDPC codes in Section III and IV, respectively. The results suggest that increasing the coupling parameter (constraint length) of the SC-LDPC code improves the diversity order of the code. A similar observation is made in [4] for the block erasure channel, which is a special case of block-fading channel.

Furthermore, we show that a higher diversity order can be achieved without decreasing the code rate R and that SC-LDPC codes are robust against the variations in the channel, e.g. a mobile-radio channel is not stationary over time and it fluctuates between the extremes of Rayleigh and AWGN channel. We support the density evolution results with simulation results for finite length codes. In Section V, a latency constrained *sliding window decoder* [5] for the SC-LDPC code is considered. It has been shown in [6] for an AWGN channel, that even for a small structural delay (< 500 bits), the windowed decoding of SC-LDPC codes outperform both conventional convolutional codes with Viterbi decoding and LDPC block codes. We consider (3,6)-regular codes as an example, which already exhibit remarkable diversity improvement. A general analytical bound on achievable diversity is hard to obtain but our experimental results indicate that better diversity can be achieved by further increasing the node degrees.

II. NON-ERGODIC BLOCK-FADING CHANNEL

We consider transmission of a codeword of length N . The slowly varying nature of the channel allows us to divide the codeword into F subblocks, of length $N_f = N/F$ each. These F subblocks are affected by different independent fading realizations $\alpha_j, j = 1, \dots, F$. The received symbols, $y_i, i = 1, \dots, N$, have the following form,

$$y_i = \alpha_j x_i + n_i, \quad (1)$$

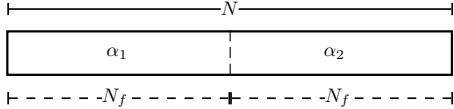


Fig. 1. Illustration of block-fading channel for a codeword of length N and $F = 2$.

where $j = 1 + \lfloor (i-1)/N_f \rfloor$ and $\lfloor \cdot \rfloor$ represents the floor operator. The input symbols x_i are chosen from BPSK alphabet and n_i are Gaussian random variables with zero mean and variance σ_n^2 . The symbols are normalized to $x_i = \pm 1$ and the fading coefficients α_j are Rayleigh distributed with $\mathbb{E}[\alpha_j^2] = 1$. Hence, the signal-to-noise ratio (SNR = γ) of the received symbols is characterized only by the variance of the Gaussian noise. Figure 1 gives an example of a codeword transmitted over two fading channels ($F = 2$). The fading values α_1 and α_2 are constant throughout the first and second half of the codeword, respectively. We further assume perfect channel information only at the receiver side¹. The log-likelihood ratio (LLR) of the received symbols y_i is given as,

$$L_i = \frac{2\alpha_j}{\sigma_n^2} y_i. \quad (2)$$

The capacity of a non-ergodic channel depends on the channel realization (here fading coefficients α_j) and hence is not information stable [7]. Therefore, the Shannon capacity of a block-fading channel is zero. In order to characterize such a channel, the *outage probability* P_{out} serves as a lower bound on the word error probability for any coding scheme. The outage probability is defined as follows [1],

$$P_{\text{out}} = \mathbb{P}(I(\mathbf{x}; \mathbf{y} | \boldsymbol{\alpha}) < R) \quad (3)$$

where $I(\cdot)$ denotes the instantaneous mutual information between the input and the output of the channel, R is the transmission rate and $\boldsymbol{\alpha} = \{\alpha_1, \dots, \alpha_F\}$. Hence, an outage occurs when the fading values in $\boldsymbol{\alpha}$ are such that the mutual information between the input and the output of the channel is below the code rate. Assuming the input symbols x_i to be binary (BPSK), the outage probability is given as, [8],

$$P_{\text{out}} = \mathbb{P} \left(\sum_{j=1}^F \mathbb{E}_X [\log_2(1 + e^{-4R\alpha_j^2 X})] > F(1 - R) \right) \quad (4)$$

with $X \sim \mathcal{N}(\gamma, \gamma)$. The P_{out} in (4) is an outage boundary for a random code and can be approximated to $2/\gamma^2$ for $R = 1/2$ code and $F = 2$ under high SNR(γ) [8]. However, in general P_{out} has no close form expression.

A. Coding for Block-Fading Channels

A code design for a block-fading channel must exploit the distinct characteristics of the channel. An important feature is that each subblock is faded by an independent fading value, providing some *diversity*. The F subblocks in a codeword are

¹If channel-state information is available at the transmitter side, fading can be compensated by controlling the transmit power accordingly.

coded together to reduce the probability of all the code symbols being faded simultaneously. At high SNR, the *diversity order* of the code defines the slope of the error rate curve on a log-log scale and is given as,

$$d = - \lim_{\gamma \rightarrow \infty} \frac{\log(P_{\text{we}})}{\log(\gamma)} \quad (5)$$

where P_{we} is the *word error probability*. A code with rate $R = 1/F$ is said to have full diversity if $d = F$. Next, we consider an LDPC block code and a spatially coupled LDPC code for block-fading channel.

III. LDPC CODES FOR BLOCK-FADING CHANNELS

A (J, K) -regular LDPC code is characterized by a sparse parity-check matrix \mathbf{H} containing exactly J and K ones in each column and row, respectively. Here, we consider protograph based LDPC codes described by a bi-adjacency matrix \mathbf{B} , called *base matrix*. A protograph is a small bipartite graph consisting of n_c check and n_v variable nodes. The parity-check matrix \mathbf{H} of an LDPC code can be obtained by applying a lifting procedure that replaces each 1 in \mathbf{B} by an $Z \times Z$ permutation matrix and each 0 by an $Z \times Z$ all-zero matrix. Integer entries larger than 1 represent multiple edges between a pair of nodes and are replaced by a sum of permutation matrices. The resultant parity-check matrix \mathbf{H} defines a codeword $\mathbf{v} = \{v_1, \dots, v_N\}$ of length $N = Zn_v$.

A. Density Evolution Outage

We use density evolution to analyze the exact performance of a random LDPC block code for a block-fading channel. Density evolution tracks the probability density function of the messages exchanged between the check and variable nodes in the bipartite graph. The worst channel parameter for which the bit error probability converges to zero is called the *threshold* of an ensemble. Here, as discussed before, the threshold of an ensemble for the block-fading channel depends on the channel realization and hence does not exist.

Considering (3), an outage occurs when instantaneous input-output mutual information is less than the transmission rate R . In terms of density evolution, we define *density evolution outage* (DEO) as an event when the bit error probability does not converge to zero for a fixed value of SNR after finite or infinite number of decoding iterations are performed [2]. The *probability of density evolution outage*, P_{DEO} , for a fixed value of SNR can then be calculated using a Monte Carlo method considering significant number of fading coefficients. The lower bound on the word error probability P_{we} is given as [2],

$$P_{\text{we}} \geq P_{\text{DEO}}. \quad (6)$$

Consider, without loss of generality, transmission of all-zero codeword and perfect channel information at the receiver side. The mean and variance of the received LLR from (2) can then be calculated as $2\alpha_j^2/\sigma_n^2$ and $4\alpha_j^2/\sigma_n^2$, respectively. Hence, the block-fading channel can be modeled as an AWGN channel with gain α_j for each subblock of length N_f symbols and the initial distribution of the received symbols is generated using

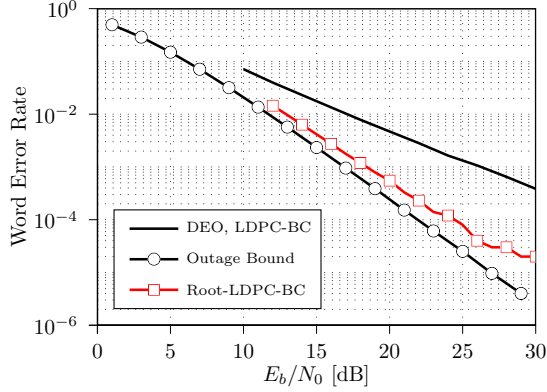


Fig. 2. Density evolution outage probability for a random (3,6)-regular LDPC block code (LDPC-BC) and for a (3,6) root-LDPC block code with $F = 2$. The outage bound calculated using (4) is also plotted.

the mean and variance of the LLR value in (2). The fading coefficient α_j can be interpreted as a known gain.

Figure 2 shows the outage probability bound for random block codes and P_{DEO} for a random (3,6)-regular LDPC codes calculated using (4) and (6), respectively. It can be observed that the LDPC block code does not achieve the outage bound and its diversity order is $d \approx 1.3$. In order to achieve full diversity $d = F = 2$, which is the maximum achievable diversity order for an $R = 1/F$ code, root-LDPC codes are introduced in [2]. The simulation result for a randomly generated (3,6)-regular root-LDPC code in Fig. 2 shows that the WER closely matches with the outage bound, corresponding to a diversity $d = 2$.

IV. SC-LDPC CODES FOR BLOCK-FADING CHANNELS

Now consider the transmission of a sequence of codewords \mathbf{v}_t , $t = 1, \dots, L$ each of length N , using a protograph based LDPC code. Instead of encoding the sequence of codewords independently, the blocks \mathbf{v}_t are *coupled* by the encoder over various other time instants [9]. The maximal distance between a pair of coupled blocks defines the memory m_{cc} of the convolutional code. The coupling of consecutive blocks can be achieved by an *edge spreading* procedure [10] that distributes the edges from variable nodes at time t among equivalent check nodes at times $t + i$, $i = 0, \dots, m_{cc}$. This procedure is illustrated in Fig. 3 for a (3,6)-regular protograph with base matrix $\mathbf{B} = [3, 3]$. In order to maintain the degree distribution and structure of the original ensemble, a valid edge spreading should satisfy the condition $\sum_{i=0}^{m_{cc}} \mathbf{B}_i = \mathbf{B}$. The resulting ensemble can be described by means of a terminated *convolutional protograph* with base matrix

$$\mathbf{B}_{[1,L]} = \begin{bmatrix} \mathbf{B}_0 & & & & & \\ \vdots & \ddots & & & & \\ \mathbf{B}_{m_{cc}} & & \mathbf{B}_0 & & & \\ & & & \ddots & & \\ & & & & \vdots & \\ & & & & & \mathbf{B}_{m_{cc}} \end{bmatrix}_{(L+m_{cc})n_c \times Ln_v} \quad (7)$$

The corresponding sequence of coupled code blocks forms a codeword $\mathbf{v}_{[1,L]} = [\mathbf{v}_1, \mathbf{v}_2, \dots, \mathbf{v}_t, \dots, \mathbf{v}_L]$ of a terminated

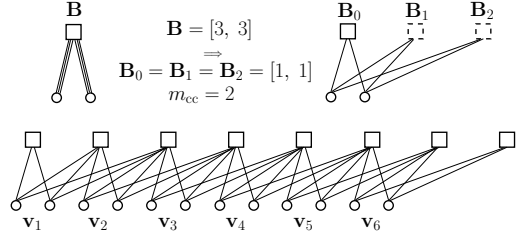


Fig. 3. Illustration of edge spreading: the protograph of a (3,6)-regular block code with base matrix \mathbf{B} is repeated $L = 6$ times and the edges are spread over time according to the component base matrices \mathbf{B}_0 , \mathbf{B}_1 , and \mathbf{B}_2 , resulting in a terminated SC-LDPC codeword $\mathbf{v}_{[1,6]} = [\mathbf{v}_1, \dots, \mathbf{v}_6]$.

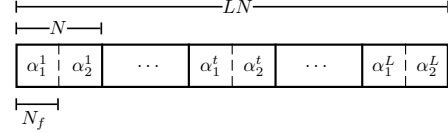


Fig. 4. Illustration of block-fading channel with $F = 2$ for a SC-LDPC codeword $\mathbf{v}_{[1,L]}$ with termination length L . The length of each coupled codeword \mathbf{v}_t is N .

SC-LDPC code. Note that the $m_{cc}n_c$ additional check nodes result in a rate loss due to termination. The block code ensemble with disconnected protographs corresponds to the special case $m_{cc} = 0$ with $\mathbf{B}_0 = \mathbf{B}$.

A. Density Evolution Outage for SC-LDPC Codes

Similar to LDPC block codes in Section III, DEO can be calculated for a SC-LDPC code represented by a coupled bipartite graph in Fig. 3. An illustration of a terminated SC-LDPC codeword $\mathbf{v}_{[1,L]} = [\mathbf{v}_1, \dots, \mathbf{v}_t, \dots, \mathbf{v}_L]$ with termination length L and $F = 2$ is given in Fig. 4. Each individual codeword \mathbf{v}_t is divided into F equal subblocks. For $F = 2$, the two fading coefficients for the first and second half (N_f bits) of the codeword \mathbf{v}_t are represented as α_1^t and α_2^t , respectively.

Since a Monte Carlo method to calculate P_{DEO} with exact density evolution for a SC-LDPC is far too complex, we use a reciprocal channel approximation (RCA) technique [11] to calculate the P_{DEO} for a fixed SNR value. In case of the BEC, density evolution can be represented by a one-dimensional parameter, i.e., erasure probability. RCA uses a one-dimensional representation per variable node for the block-fading channel. The one-dimensional parameter within the RCA method is the mean of the received LLR symbol given by (2) and depends on the particular fading realization.

A check node at time t in a SC-LDPC code is connected to $m_{cc} + 1$ codewords \mathbf{v}_{t-i} , $i = 0, \dots, m_{cc}$ as shown in Fig. 3. Considering the block-fading model in Fig. 4, a codeword \mathbf{v}_t has F independent fading values. Hence, each check node in the coupled graph is connected to at most $F(m_{cc} + 1)$ independent fading coefficients. Therefore, for a fixed channel parameter F , the diversity order can be increased by increasing m_{cc} of the coupled code, while keeping R and F same.

The component matrices for a (3,6)-regular SC-LDPC code with an increasing memory $m_{cc} = 1, \dots, 4$ are considered in Table I. Figure 5 shows the corresponding DEO probabilities determined using (6) and RCA approximation. The diversity

TABLE I
THE COMPONENT MATRICES FOR THE EDGE SPREADING PROCEDURE
USED FOR (3,6)-REGULAR SC-LDPC CODE. THE DIVERSITY ORDER IS
CALCULATED FOR $F = 2$.

Ensemble	m_{cc}	$\mathbf{B}_i, i = 0, \dots, m_{cc}$	d
LDPC-BC	0	$\mathbf{B} = \mathbf{B}_0 = [3, 3]$	1.3
EnsA1	1	$\mathbf{B}_0 = [2, 2], \mathbf{B}_1 = [1, 1]$	3
EnsA2	2	$\mathbf{B}_{0,1,2} = [1, 1]$	6
EnsA3	3	$\mathbf{B}_{0,3} = [1, 1], \mathbf{B}_1 = [1, 0], \mathbf{B}_2 = [0, 1]$	10
EnsA4	4	$\mathbf{B}_0 = [1, 1], \mathbf{B}_{1,3} = [1, 0], \mathbf{B}_{2,4} = [0, 1]$	10

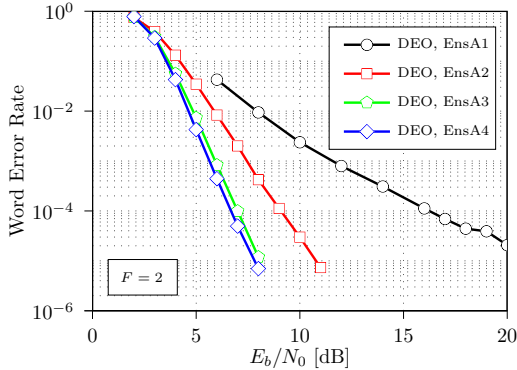


Fig. 5. DEO probability for ensembles defined in Table I.

order for the ensembles in Table I is numerically computed from Fig. 5. The diversity order of the code increases with the coupling parameter m_{cc} . We observe that even a coupling to one neighboring block ($m_{cc} = 1$) gives a diversity order of 3, which is more than twice as compared to the LDPC block code (see Fig. 2). Furthermore, increasing the memory of the code from 3 to 4 does not give any significant improvement in the diversity order. This is due to the fact that the maximum number of codewords connected to a check node is limited by the memory and the node degree. Hence, only simultaneously increasing node degree and memory would result in increase in the diversity order of the ensemble.

Considering EnsA2 as an example, the diversity order of the code is $d = 6$ with $R = 1/2$. As shown in Fig. 6, the same diversity can be achieved with a block code in case of $F = 10$ according to the outage bound, as calculated using (4). The results suggest that in order to achieve the same performance with a random block code of $R = 1/2$ and optimal maximum likelihood decoding, a codeword of length $N = 10N_f$ ($F = 10$) must be considered. Note that from Fig. 2, we can conclude that a random LDPC block code with $N = 10N_f$ will not reach this outage bound. However, a full-diversity root-LDPC code with $d = 6$ is possible to design but only with a rate $R = 1/d = 1/6$. In contrast to this, at the expense of slight rate loss due to termination, a randomly generated (3,6)-regular SC-LDPC code with $m_{cc} = 2$ is sufficient to achieve the diversity order of $d = 6$. Likewise, in order to achieve the diversity order of $d = 10$, similar to

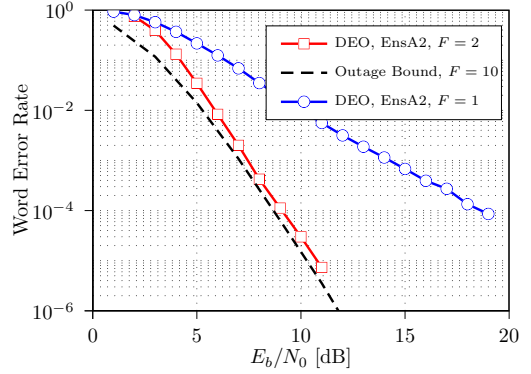


Fig. 6. DEO probability for EnsA2 for $F = 1$ and 2. The outage bound for block code (4) is also plotted for $F = 10$.

EnsA3 and EnsA4 (see Table I), a rate $R = 1/2$ random block code with $F = 16$ is required (curve not shown here).

Figure 6 also shows the DEO probability for $F = 1$, where $N = N_f$. The diversity order of EnsA2 reduces to 3. Whereas, a block code with $R = 1/2$ or a root-LDPC code designed for $F = 2$ would have a maximum diversity of $d = 1^2$. This suggests that the SC-LDPC codes are more robust against the variation in the channel parameter F compared to root-LDPC codes, i.e., designing a code for a specific value of F is not required and the diversity order strongly depends on the memory of the code. We observed that as long as the constraint length of the code $N(m_{cc} + 1)$ contains more than one subblock of length N_f , the SC-LDPC code can provide a diversity order greater than 1. However, so far we have not been able to give any bound on the diversity of a SC-LDPC code with respect to the coupling parameter and more analysis is required.

B. Simulation Results

We demonstrate the results of WER for finite length codes generated randomly while avoiding the cycles of length 4. The block length of each individual coupled code \mathbf{v}_i is $N = 200$ and $F = 2$. A maximum number of 50 iterations are performed and the iterations stop once the check nodes are fulfilled. Figure 7 shows the simulated WER for EnsA1, EnsA2 and EnsA4 together with the DEO probabilities from Fig. 5. We observe that there is no significant difference between the DEO probability and the simulated WER for a finite block length N . Note that, density evolution assumes an infinite block length.

V. LATENCY CONSTRAINED DECODING OF SC-LDPC CODES

So far, we presented the results when standard belief propagation decoding is applied across the codeword $\mathbf{v}_{[1,L]}$. This induces a large structural decoding delay of LN code bits. The structural delay is defined as the number of code bits, the decoder has to wait before starting the decoding process. In order to limit the decoding latency, we use a *sliding windowed decoder* of size W introduced in [5].

²using Singleton-like bound [12] on diversity order $d \leq 1 + \lfloor F(1 - R) \rfloor$

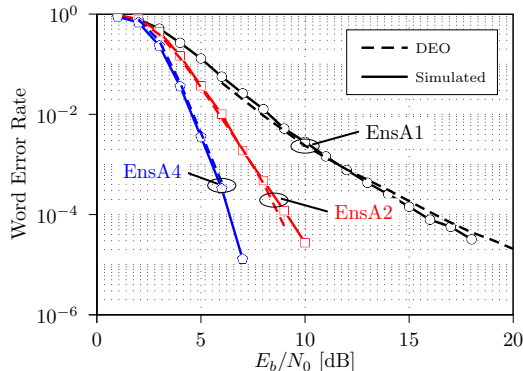


Fig. 7. Simulated WER and DEO probabilities for EnsA1, EnsA2 and EnsA4, $N = 200$, $L = 100$, $F = 2$.

A window at time t operates on W received words, $\mathbf{y}_t, \mathbf{y}_{t+1}, \dots, \mathbf{y}_{t+W-1}$, corresponding to a section of Wn_c rows and Wn_v columns of the matrix in (7). The size of the window decoder is limited by at least $m_{cc} + 1$ codewords, which is the maximal distance between two coupled codewords. At window position t , only symbols in \mathbf{y}_t are decoded and hence termed as *target symbols*. After the received word \mathbf{y}_t is decoded or the maximum number of iterations are performed, the window slides n_c rows down and n_v columns right in $\mathbf{B}_{[1,L]}$. By using a window decoder, the structural latency is reduced to WN , where in general $W \ll L$.

The window decoder of size W is applied to the same codes used in Fig. 7. A maximum number of 50 iterations are performed at each window position. We compare the results for EnsA1 and EnsA2 for different window sizes. The edge spreading in EnsA1 containing multiple edges in \mathbf{B}_0 is considered as this achieves the target BER with smaller W [5] for an AWGN and BEC channel. Note that the structural latency is proportional to W and hence a small value of W is desirable for latency constrained applications.

Figure 8 shows the WER when a window decoder is used to decode a SC-LDPC code. The corresponding DEO probabilities from Fig. 5 are also plotted as reference. We define W_{\min} as the minimum window size required to obtain the performance of a belief propagation decoder that is applied across the entire coupled codewords $\mathbf{v}_{[1,L]}$ (this corresponds to results presented in Section IV). A window size of $W_{\min} = 5$ is sufficient for EnsA1 (double edges in \mathbf{B}_0) whereas, a $W_{\min} = 10$ is required for EnsA2 to achieve the respective DEO probability. This can be explained due to the degree-one variable nodes at the right end of window in EnsA2. However, our results show that the window decoder with size $W < W_{\min}$ for EnsA2 performs better than EnsA1 with $W = W_{\min}$, although the latter contains double edges in \mathbf{B}_0 . This can be explained by the difference in memory of the two ensembles, since the number of different (independent) fading values connected to any check node in a graph is proportional to the memory of the code (see Fig. 3). Hence, we can conclude that the word error performance of a window decoder depends strongly on the coupling parameter m_{cc} rather than the edge spreading used.

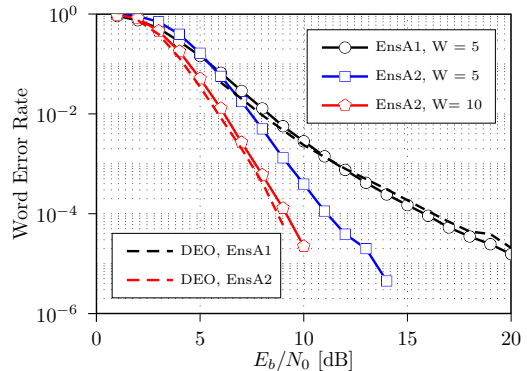


Fig. 8. Simulated WER and DEO for EnsA1 and EnsA2 using window decoder of size W , $N = 200$, $L = 100$, $F = 2$.

VI. CONCLUSION

We present DEO probabilities and simulation results on finite length SC-LDPC codes for the block-fading channel. A simple (3,6)-regular SC-LDPC codes have been demonstrated to achieve a diversity order of $d = 10$. We demonstrate that SC-LDPC codes do not require channel specific design and the increase in diversity order depends on the coupling parameter m_{cc} of the code. While root-LDPC codes have to be designed specifically for a given F , the SC-LDPC codes are more robust against variation in the fading channel. Furthermore, a latency constrained decoding of SC-LDPC codes using a window decoder gives no significant loss in word error performance compared to a block decoder.

REFERENCES

- [1] L. Ozarow, S. Shamai (Shitz), and A. Wyner, "Information theoretic considerations for cellular mobile radio," *IEEE Transactions on Vehicular Technology*, vol. 43, no. 2, pp. 359–378, 1994.
- [2] J. Boutros, A. Guillen i Fabregas, E. Biglieri, and G. Zemor, "Low-density parity-check codes for nonergodic block-fading channels," *IEEE Trans. on Inf. Theory*, vol. 56, no. 9, pp. 4286–4300, 2010.
- [3] E. Biglieri, G. Caire, and G. Taricco, "Coding for the fading channel: a survey," *Signal Processing*, vol. 80, no. 7, pp. 1135–1148, 2000.
- [4] A. Jule and I. Andriyanova, "Performance bounds for spatially-coupled LDPC codes over the block erasure channel," in *Proc. of IEEE International Symposium on Information Theory*, Jan. 2013, pp. 1879–1883.
- [5] M. Papaleo, A. Iyengar, P. Siegel, J. Wolf, and G. Corazza, "Windowed erasure decoding of LDPC convolutional codes," in *Proc. IEEE Information Theory Workshop (ITW)*, Jan. 2010, pp. 1–5.
- [6] N. Ul Hassan, M. Lentmaier, and G. Fettweis, "Comparison of LDPC block and LDPC convolutional codes based on their decoding latency," in *Proc. 7th International Symposium on Turbo Codes & Iterative Information Processing*, Aug. 2012, pp. 225–229.
- [7] S. Verdú and T. Han, "A general formula for channel capacity," *IEEE Trans. on Inf. Theory*, vol. 40, no. 4, pp. 1147–1157, 1994.
- [8] I. Andriyanova, E. Biglieri, and J. Boutros, "On iterative performance of LDPC and Root-LDPC codes over block-fading channels," in *Proc. 48th Annual Allerton Conference on Communication, Control, and Computing (Allerton)*, 2010, pp. 167–171.
- [9] A. Jimenez Felstrom and K. Zigangirov, "Time-varying periodic convolutional codes with low-density parity-check matrix," *IEEE Trans. Inf. Theory*, vol. 45, no. 6, pp. 2181–2191, Sep. 1999.
- [10] M. Lentmaier, G. Fettweis, K. Zigangirov, and D. Costello, "Approaching capacity with asymptotically regular LDPC codes," in *Proc. Information Theory and Applications Workshop*, Feb. 2009, pp. 173–177.
- [11] S.-Y. Chung, "On the construction of some capacity-approaching coding schemes," Ph.D. dissertation, Massachusetts Institute of Technology, Cambridge, MA, 2000.
- [12] R. Knopp and P. Humblet, "On coding for block fading channels," *IEEE Trans. on Inf. Theory*, vol. 46, no. 1, pp. 189–205, 2000.